Preparation of Poly(styrene-*co*-butyl acrylate)/ Montmorillonite Nanocomposite by Emulsion Polymerization: Characterization and Nanoscratch Behavior

M.R. Moghbeli, N. Mehdizadeh

Petrochemical Department, School of Chemical Engineering, Iran University of Science and Technology (IUST), Tehran, Iran

Received 8 January 2011; accepted 9 April 2011
DOI 10.1002/app.34721
Published online 23 August 2011 in Wiley Online Library (wileyonlinelibrary.com).

ABSTRACT: Organic–inorganic hybrid poly(styrene-*co*-butyl acrylate)/organically modified montmorillonite (PSBA/organo-MMT) latex particles have been prepared by *in situ* emulsion polymerization. The effects of modifier variety and the level of organo-MMT have been investigated on the basis of the characteristics and mechanical properties of the resulting hybrid emulsion polymers. Although the more hydrophilic intercalated organic modifiers increased the latex particle size, the hydrophobic ones decreased the particle size. A more heterogeneous copolymer chain intercalation was seen by widespread XRD reflection as the organo-MMT (organoclay) level increases. The tapping mode atomic force microscopy (AFM) and transmission electron microscopy (TEM) were used to determine the dispersion state of organoclay particles inside the nanocomposite copolymer films. Dynamic mechanical thermal analysis (DMTA) showed that adding the organoclay to the copolymer decreased the maximum loss tangent (tanδ) value and caused the shift to a lower temperature. Interestingly, the incorporation of organoclay decreased the glass storage modulus of the copolymer, while increased the rubbery storage modulus to some extent. In addition, a standard indenter for the nanoscratching of copolymer nanocomposite films was used under low applied loads of 150 and 250 μ*N*. The nanoscratch results showed that incorporation of a 3 wt % hydrophobic organoclay, e.g., Closite15A, in the copolymer matrix enhanced considerably the near-surface hardness and grooving resistance of the nanocomposite film at room temperature. In fact, copolymer nanocomposite films with higher near-surface hardness and tanδ curve broadening exhibited more nanoscratch resistance through a specific variety of viscoelastic deformation, which did not create a bigger groove.
 J Appl Polym Sci 123: 2064–2073, 2012

Key words: *in situ* emulsion polymerization; montmorillonite; nanocomposite; nanoscratching; poly (styrene-*co*-butyl acrylate)

INTRODUCTION

The presence of a small amount of high-strength inorganic nanofillers with a high aspect ratio, such as layered silicates, and carbon nanotubes (CNTs), could enhance the physical and the mechanical properties of thermoplastic materials. [1–5] A serious problem related to the use of nanosized hydrophilic fillers is their homogeneous dispersion within the organic matrix, thereby leading to macroscopic phase separation.[6] Even when the particles are well dispersed in the matrix, nanoparticle aggregation may occur during processing and may seriously deteriorate the physical and mechanical properties. A common method to prevent this undesirable occurrence is surface treatment of nanoparticles with organic surfactants or organosilane coupling agents.[7–9] This treatment improves the compatibility between the polymer and the nanoparticle, and increases the opening distance between clay silicate layers to facilitate the monomer or the polymer inclusion in between.[10–11] On the other hand, polymerizing monomers inside the organoclay galleries by emulsion polymerization is one of the approaches to prepare more homogeneous reinforced polymer systems.[12,13] Choi et al.[14] have investigated the chemical affinity between a monomer mixture and an organoclay by varying the initial composition of the feed monomer used in an emulsion polymerization.

Kim et al.[15] synthesized exfoliated polystyrene/sodium montmorillonite (PS/Na-MMT) emulsion nanocomposites containing 3 wt % of Na-MMT using a reactive surfactant, that is, 2-acrylamido-2-methyl-1-propane sulfonic acid (AMPS), and dodecylbenzenesulfonic acid sodium salt (DBS-Na). As a reactive surfactant, AMPS makes the polymer tether to the end of the pristine Na-MMT clay surface. Zhang and Wilkie[16] used carbocation-substituted clay to prepare PS/org-MMT nanocomposites with higher thermal stability. Yei et al.[17] enhanced thermal properties of the PS nanocomposites formed

Correspondence to: M.R. Moghbeli (mr_moghbeli@iust.ac.ir).

from inorganic (aminopropulisobutyl polyhedral oligomeric silsesquioxane) POSS-treated montmorillonite. Using this type of *in situ* surfactant resulted in an exfoliated nanocomposite. Aphiwantrakul et al.[18] have investigated the effect of cation exchange capacity (CEC) of the clay on the physical and the mechanical properties of polystyrene–clay nanocomposites prepared by *in situ* intercalative polymerization. In this case, the surface density of modifier depends on the CEC of the clay used. Li et al.[19] synthesized exfoliated polystyrene/montmorillonite nanocomposite by emulsion polymerization using a dipole ion amino acid, i.e., aminoundecanoic acid (AUA), as a clay modifier. Zhanga et al.[20,21] prepared graphite-oxide-reinforced poly(styrene-*co*-butyl acrylate) to improve flammability and thermal stability of the resulting nanocomposite prepared in an emulsion polymerization. Sahoo and Samal[22] used Na-MMT directly without any surface treatment to synthesize the poly(methyl methacrylate)/Na-MMT nanocomposite. Their results showed that an exfoliated structure for the nanocomposite with 5 wt % Na-MMT. A hybrid poly(styrene-*co*-butyl acrylate)-Brazilian montmorillonite was prepared by miniemulsion polymerization by Moraes et al.[23]

Recently, nanoparticles such as clays and nanofibers have been used to improve the surface and near-surface mechanical properties of the polymer coatings.[24–28] For this purpose, nanoscratching has been used to evaluate the scratch resistance, wear, and friction behaviors of the polymer-based nanocomposites to a lesser extent. Amerio et al.[29] investigated the effect of inorganic silica domains, introduced either by dispersing preformed silica nanoparticles or by *in situ* generation by sol–gel, on the scratch behavior of reinforced acrylic coatings. Their results showed that scratch resistance of the coatings obtained by sol–gel dual curing process is considerably higher than that of the coatings prepared by dispersing preformed nanosilica into the acrylic resin. The effect of nanoclay on the scratch-deformed region and starch resistance of the semicrystalline polymers has been investigated.[30,31] In this case, introduction of nanoclay significantly reduced the severity of the scratch-deformed region and decreased the volume of nanofillers formed in the nanocomposite films.

Although some scientists have investigated the effect of clay level and surface treatment on the mechanical properties of the polymers, less attention has been paid to the investigation of the effect of organoclay on the nanoscratching of styrenic copolymer nanocomposites prepared by *in situ* emulsion polymerization. In the present research, the effects of the surface modifier variety and the level of the organo-MMT on the dynamic mechanical thermal properties and nanoscratching of poly(styrene-*co*-butyl acrylate) have been investigated.

TABLE I
Characteristics of the Pristine Sodium Montmorillonite (NaMMT) and Organically Modified Montmorillonites (organo-MMTs)

Clay	Modifier[a]	2θ (°)	*d*-spacing (Å)
ClositeNa+	–	8.83	10.0
Closite15A	2M2HT	2.78	31.7
Closite30B	MT2EtOH	6.25	14.2
AUA-Clay	AUA	6.46	13.7

[a] The clay surface modifier of Closite15A (C15A), Closite30B (C30B), and AUA-Clay are dimethyl dehydrogenated tallow (2M2HT), methyl tallow bis-2-hydroxyethyl ammonium (MT2EtOH), and aminoundecanoic acid (AUA), respectively.

EXPERIMENTAL

Materials

All reagents were purchased from Merck unless otherwise stated. Styrene (St) and butyl acrylate (BA) were distillated under vacuum to remove the inhibitor and held at +5°C before use. Potassium persulfate (KPS), sodium dodecyl sulfate (SDS), acetone, tetrahydrofuran (THF), and 1, 1-aminoundecanoic acid (AUA) (Fluka) were used without any further purification. Twice-distillated water was prepared in the author's lab. The natural Na-MMT, cation exchange capacity (CEC): 95 meq/100 g, Closite15A (C15A), and Closite30B (C30B) were prepared from Southern Clay (USA). In addition, the Na-MMT was modified with 1.5 CEC AUA modifier through the procedure reported previously. [15] In this case, the modified clay was designated as AUA-clay. The type and chemical structure of all modifiers used were listed in Table I.

Emulsion polymerization

The free radical emulsion polymerization of styrene/butyl acrylate (60/40 by weight) in the presence of 1 and 3 wt % organoclay, i.e., C15A, C30B, or AUA-clay, was carried out in a glass reactor equipped with a reflux condenser and a nitrogen inlet. First, the organoclay was preswelled by a monomer mixture overnight under vigorous mixing, i.e. 2000 rpm, and then added to the reactor. The reaction mixture was maintained at 70°C and stirred mechanically at 300 rpm under nitrogen atmosphere. The polymerization was conducted in a batch process under thermostatic control and continued for 180 min. The glass reactor was immediately cooled in an ice-water-salt mixture to stop the polymerization after 180 min. The neat and hybrid copolymer latexes were synthesized according to the emulsion procedures listed in Table II. The synthesized PSBA/ organo-MMT nanocomposites were

TABLE II
Procedures for the Preparation of Hybrid Latexes

Ingredients[a]	NC1	NC2	NC3
St	12	12	12
BA	8	8	8
DDI	80	80	80
KPS	0.1	0.1	0.1
SDS	0.2	0.2	0.2
Closite15A	Variable	–	–
Closite30B	–	Variable	–
AUA-clay[b]	–	–	Variable

[a] Quantities are in weight parts (g).
[b] AUA-clay: surface-treated pristine clay with AUA.

designated with a common name (NC), followed by a code number 1, 2, or 3 which shows the nanocomposite sample contains various amount of C15A, C30B, or AUA-clay organoclays, respectively.

Nanocomposite characterization

The particle size and the size distribution of the hybrid latexes were measured by dynamic laser light scattering with a wavelength of 632.8 nm and a laser source light He and Ne gas. Light scattering measurements were performed using a Sematech SEM-633 steppermotor-driven goniometer. Overall conversion of the prepared latexes was measured gravimetrically.

The molecular weights and molecular weight distribution of the PSBA copolymer and its nanocomposites containing 3 wt % oganoclay were measured with a gel permeation chromatography (GPC) apparatus (Shimadzu, Tokyo, Japan) equipped with a refractive-index detector. The sample of dried copolymer or nanocomposite film, each 0.25 g, was added to 25 mL THF, and stirred at 300 rpm and room temperature for 48 h. Then samples were centrifuged at 5000 rpm for 1 h. The supernatant phase was separated from the sediment phase and dried under vacuum to be used to molecular weight measurement.

X-ray diffraction (XRD) (FK60-04) experiments were carried out to investigate the structure of organoclays and copolymer/organoclay nanocomposites. Dispersion state of the organoclay within the copolymer matrix was investigated by an atomic force microscopy (AFM) (Nanoscope III, Digital Instrument) apparatus. The transmission electron microscopy Zeiss CEM 902A was also used to investigate the composite structure and observe the dispersion state of the organo-MMT inside copolymer matrix. The ultrathin sections of the samples were prepared and transferred onto the mesh 400 copper grids and dried in open air before microscopy for 2 h.

Nanoscratch tests were carried out on the films cast on glass substrates using a depth-sensing nano-indentation system (Triboscope, Hysitron) capable of recording the lateral force and measuring the other near-surface properties of the films scratched at room temperature. Three nanoscratch tests were carried out on each sample. Dynamic mechanical properties of the nanocomposites were determined by means of a dynamic mechanical thermal analysis (DMTA) (PL, UK) apparatus. The prepared films (10 $\times$ 2 $\times$ 50 mm^3) were tested at a heating ramp +5°C under a fixed frequency mode of 1 Hz. The glass-rubber transition temperature (T_g) of the copolymer samples was determined based on maximum loss tangent.

RESULTS AND DISCUSSION

XRD patterns of pristine Na-MMT and organomodified montmorillonites (organo-MMTs) having different surface-modified characteristics are shown in Figure 1. Intercalation of modifier molecules between the clay silicate layers resulted in a higher interlayer opening when compared to the unmodified clay. Thus, the intercalated modifier shifted the maximum intensity peak of modified clay to a lower 2θ angle as compared to the pristine clay (Fig. 1). In fact, the increase of the opening depends on the molecular size of the modifier intercalated. Two large hydrocarbon chains of dimethyl dehydrogenated tallow (2M2HT) modifier in the C15A organoclay resulted in the highest basal spacing, 31.7 Å, whilst the lowest spacing, 13.7 Å, corresponds to the clay which was modified by 1, 1-aminoundecanoic acid (AUA) modifier (Table I). The free-radical emulsion polymerization of styrene/butyl acrylate (St/BA) monomer in the presence of Na-MMT resulted in an

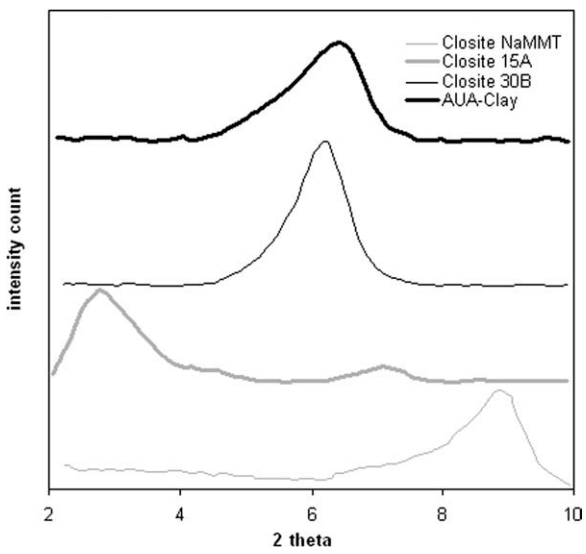

Figure 1 XRD patterns of the pristine and organomodified montmorillonites.

TABLE III
Characteristics of PSBA/Organo-MMT Hybrid Emulsions Prepared by Emulsion Polymerization

Sample	Clay	Size (nm)	M_n (kg mol^{-1})	M_w (kg mol^{-1})	PDI	T_g (°C)	2θ (°)	d_{spa} (Å)	Δ (Å)
PSBA	–	89	67.2	127.6	1.90	53	–	–	–
PSBA/15A (1%)	Closite15A	84	–	–	–	47	2.55	34.6	2.80
PSBA/15A (3%)	Closite15A	79	58.5	113.1	1.93	49	2.66	33.2	1.45
PSBA/30B (1%)	Closite30B	102	–	–	–	49	4.17	21.2	7.05
PSBA/30B (3%)	Closite30B	116	86.3	143.8	1.70	51	4.33	20.4	6.00
PSBA/AUA (1%)	AUA-Clay	109	–	–	-	47	3.86	22.9	9.20
PSBA/AUA (3%)	AUA-Clay	113	72.4	121.2	1.67	50	4.77	18.5	4.80

[a] d_{spa}: $d_{spacing}$; M_n, number-average molecular weight; M_w, weight-average molecular weight; PDI: polydispersity index is equal to M_w/M_n.

unstable emulsion product. Thus, stabilized PSBA/organo-MMT nanocomposite latexes utilizing various levels of organoclays were prepared in a batch emulsion polymerization process. The overall conversion of the prepared latexes was in the range of 96–98%.

Effect of organoclay on the latex particle size

The characteristics of the resulting emulsions are shown in Table III. As one can observe, the incorporation of C15A organoclay in the structure of resultant hybrid latex particles decreased the mean particle size to some extent as compared to the particle size of the neat copolymer latexes. In fact, the C15A organoclay's modifier (2M2HT) with lower hydrophilicity as cosurfactant would decrease the size of resulting hybrid emulsion particles. On the other hand, more hydrophilic surface modifiers, i.e., methyl tallow bis-2-hydroxyethyl ammonium (MT2EtOH) and amino-undecanoic acid (AUA), respectively, intercalated within the C30B and AUA-clay, increased the mean particle size of their corresponding hybrid latex particles. For instance, increasing the C30B level from 1 to 3 wt % increased the mean particle size from 102 to 116 nm. This behavior can be attributed to the differences in the compatibility between the monomer and the organoclay used.

Effect of organoclay on the molecular weight and T_g of copolymer

The effect of organoclay type on the molecular characteristics of the PSBA copolymer is shown in Table III. As it is shown, the incorporation of 3 wt % C30B increased the weight-average molecular weight of the copolymer from 127.6 to 163.8 kg mol^{-1}. Nevertheless, using the other organoclays decreased the molecular weight on some extent. In addition, a decrease in the glass-transition temperature (T_g) was observed for all the organoclay-reinforced copolymers when compared with the neat copolymer. The probable decrease in the molecular weight of copolymer chains within organoclay galleries, and copolymer chain slippage over the organoclay particles may reduce the T_g of the nanocomposite.

Nanostructure of organoclay-reinforced copolymer

XRD results revealed an intercalated nanocomposite structure for all the organoclay-reinforced copolymers (Table III). As shown, an increase in the organoclay interlayer spacing after polymerizing St/BA monomer mixture was observed because of the copolymer chain intercalation within the montmorillonite galleries. The highest *d*-spacing change (Δ = 9.2 Å) was observed for the nanocomposite sample containing 1 wt % AUA-clay (Table III). A higher tendency between the copolymer chains and the organoclay led to a higher *d*-spacing increase. Increasing organoclay level from 1 to 3 wt % decreased interlayer opening for all the nanocomposite samples due to organoclay agglomeration. In fact, the organoclay agglomeration prevents uniform swelling of monomer mixture into the silicate layers of organoclay. Thus, a heterogeneous polymer chain intercalation can be seen by widespread XRD reflection as the organoclay level increases (Fig. 2). In this

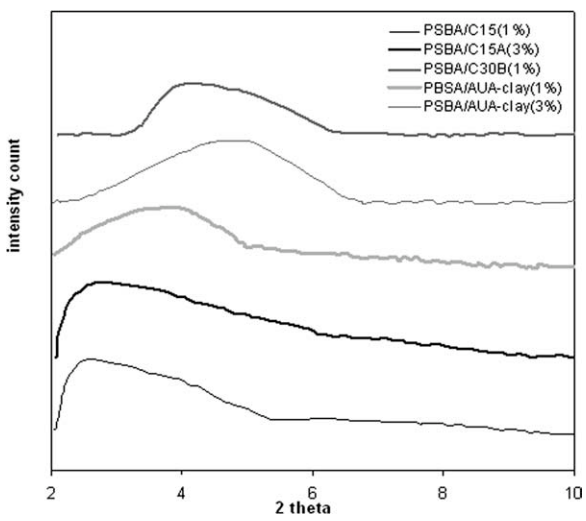

Figure 2 XRD patterns of PSBA/organo-MMT nanocomposites prepared by emulsion polymerization.

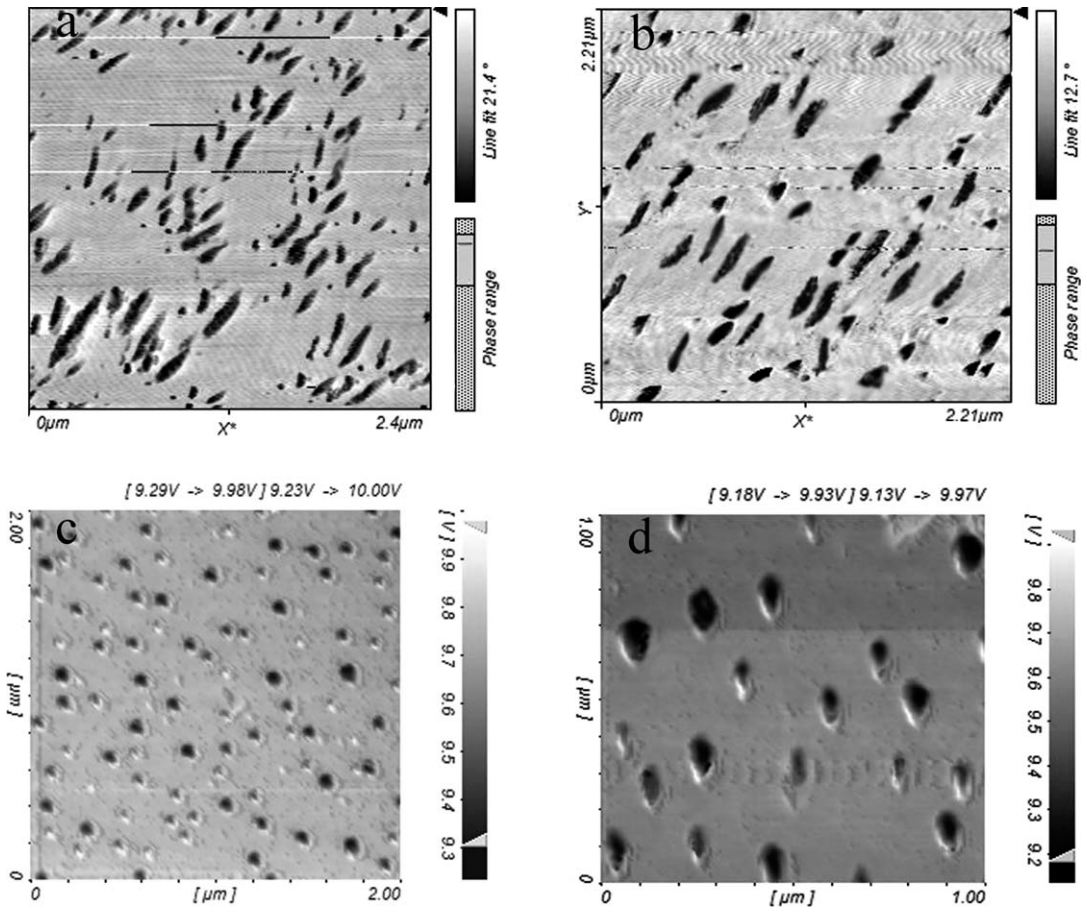

Figure 3 AFM phase image of copolymer nanocomposites containing 1 wt %: (a) C15A, (b) C30B, and (c, d) AUA-Clay.

case, the lowest interlayer opening change ($\Delta = 1.45$ Å) was observed for the copolymer nanocomposite containing 3 wt % C15A.

Nanocomposite morphology

Tapping mode atomic force microscopy (AFM) was used to determine the dispersion state of organoclay particles inside the copolymer matrix. This technique is a very sensitive tool for evaluation of local properties of materials and provides enhanced image contrast. [32–33] AFM phase micrographs show a rather uniform dispersion of organoclay particles dispersed in the nanocomposites containing 1 wt % organoclay (Fig. 3). However, the observed morphologies confirmed the intercalated nanocomposite structure composed of small organoclay tactiods well dispersed in the copolymer matrix. In this case, the average length and the thickness of the tactiods were determined based on the observed AFM micrographs as listed in Table IV. As indicated, the highest aspect ratio related to the PSBA/C15A nanocomposite varied in the range of 2–50. A very small aspect ratio belongs to the nanocomposite sample containing AUA-clay. Preparation of initial monomer/organoclay premix under long-time vigorous mechanical mixing followed by ultrasonic homogenization may break the organoclay silicate layers to very small platelets with low aspect ratio. However, some of the silicate layers of the organoclay particles with bigger length and thickness than the polymer particle size (Tables III–IV) seem to be on the surface of polymer particles or in the aqueous phase of hybrid latexes.

Figures 4–5 show the TEM micrographs of the PSBA copolymer containing 1 and 3 wt % organoclays. The stacked silicate layers of C15A and C30B are randomly dispersed in the copolymer matrix containing 1 and 3 wt % organoclay (Figs. 4–5).

TABLE IV
Length, Thickness, Aspect Ratio, and Number of Silicate Layers of the Organoclay Particles Dispersed Within the Copolymer Matrix

Sample	Length (nm)	Thickness (nm)	Aspect ratio	Number of layers
PSBA/15A(1%)	20–500	10–85	2.0–50	3–25
PSBA/30B(1%)	20–400	15–85	1.5–27	7–40
PSBA/AUA(1%)	0–160	50–100	1.6–3.2	22–44

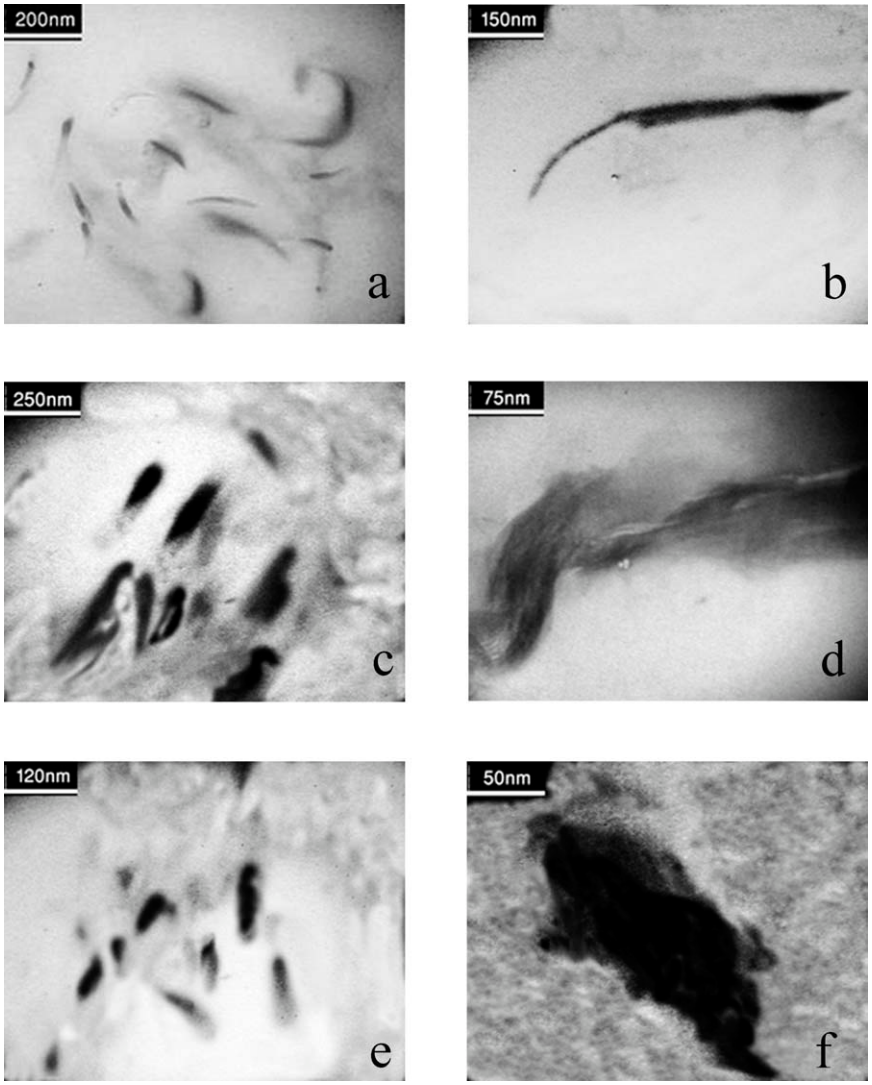

Figure 4 TEM micrographs of PSBA copolymer contain 1 wt % organo-MMTs: (a, b) C15A, (c, d) C30B, and (e, f) AUA-Clay.

However, the thickness of dispersed stacked layers of C30B is higher than that of the C15A organoclay. At higher magnification, the intercalated layers were also observed. Increasing the organoclay level from 1 to 3 wt % resulted in a more heterogeneous nanocomposite structure, exhibits some particles agglomeration in the copolymer matrix containing C30B and AUA-clay [Fig. 5(c–e)]. The lower compatibility between AUA-modified clay and PSBA copolymer resulted in a poor dispersion of silicate layers and consequently particles agglomeration inside the matrix.

Mechanical properties of nanocomposites

Dynamic mechanical properties

Dynamic mechanical behavior of nanocomposite films containing 1 and 3 wt % organoclay is shown in Figure 6. Introduction of organo-MMT particles with different surface modifiers decreased the glassy storage modulus of the copolymer, while increased the rubbery storage modulus to some extent. Figure 7 shows the tan δ curves of the neat copolymer and the organoclay-reinforced copolymers versus temperature. As one can observe, the neat copolymer itself has a slightly higher glass-rubber transition temperature about 52°C with a sharp tan δ value. Adding the organoclay to the copolymer lowered considerably the maximum tan δ and shifted it to a lower temperature, except for the nanocomposite samples containing C30B. In addition, for the aforementioned nanocomposites having a rather good organoclay dispersion state, a higher maximum tanδ was observed when compared with the other nanocomposite samples. In contrast, the lower interfacial interaction in the PSBA/C15A nanocomposite samples seems to push heterogeneous molecular

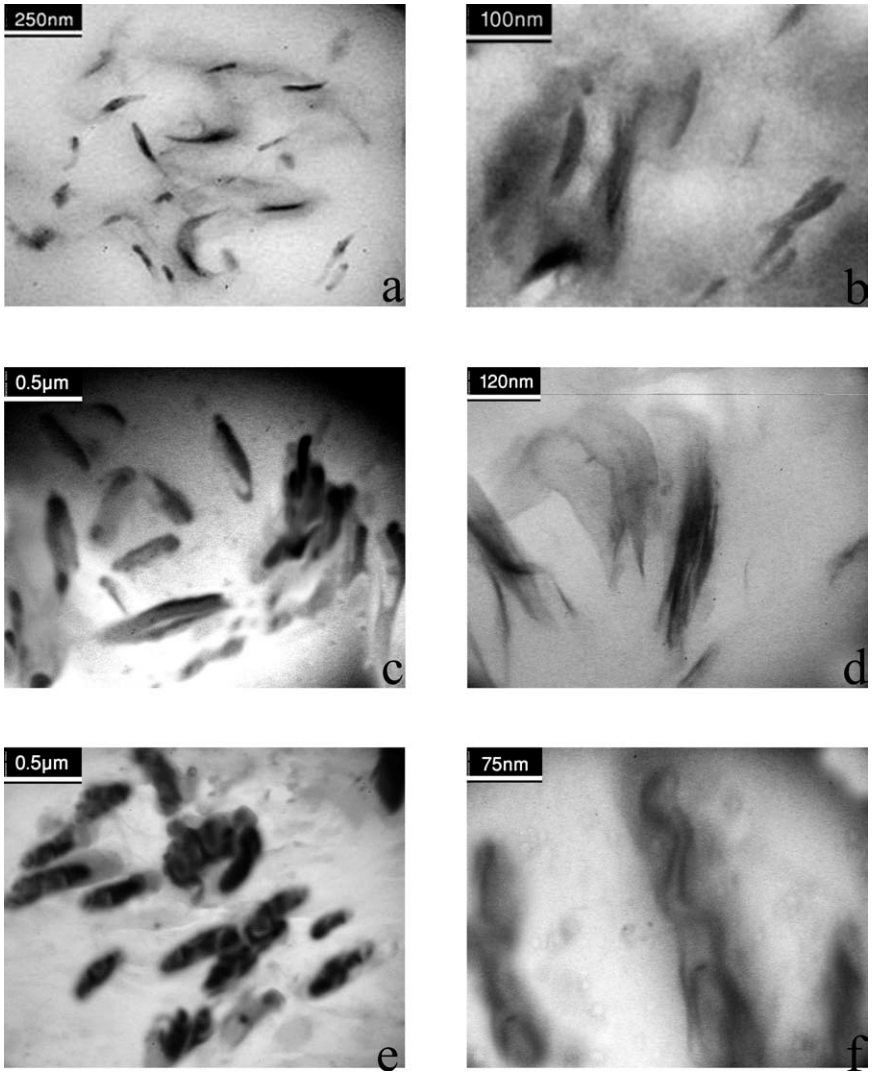

Figure 5 TEM micrographs of PSBA copolymer contain 3 wt % organo-MMTs: (a, b) C15A, (c, d) C30B, and (e, f) AUA-Clay.

motions and copolymer chain slippage over the organoclay particles, indicating a lower tan δ value and a greater half-height width of tanδ curve (Fig. 7). The tan δ width and height depends upon the heterogeneity of composition and weight fraction of each dynamic area, respectively. On the other hand, low molecular weight copolymer chain confined within the organoclay galleries as well as the chain slippage over the organoclay particles may present new motional components to the dynamic response of the sample that leads to local environmental heterogeneity and curve broadening.

Nanoscratch behavior

The nanocomposite films prepared with 1 and 3 wt % organoclay were scratched under normal loads of 150 and 250 μ*N*. Three-dimensional (3D) AFM images show the nanoscratch groove for the neat copolymer and its nanocomposites with 1 and 3 wt % organoclay (Fig. 8). As shown, a periodic pattern of plastic deformation on the wall of grooves was observed for all the samples. This behavior can be attributed to the stick-slip process that occurred during plugging of the copolymer film. Nanoscratching of the copolymer films resulted in a pile up of material pushed to the groove edges. For the organoclay nanocomposites, the lowest pushed material was observed for the sample containing C15A organoclay [Fig. 8(b)]. An increase in organoclay level from 1 to 3 wt % exhibited a lower grooving and pushed material.

The residual depth pattern on the bottom of the nanoscratch groove is shown in Figure 9. For the neat copolymer, a smooth residual depth pattern was observed, while the incorporation of organoclay in the copolymer resulted in a rough residual depth, indicating a more plastic deformation.

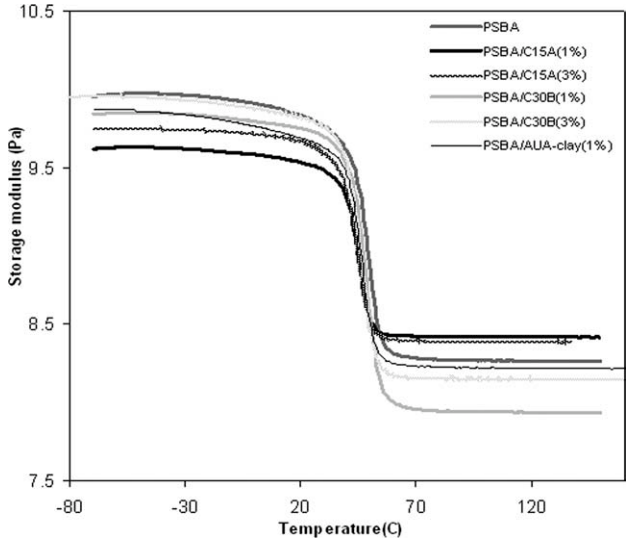

Figure 6 Temperature-dependence storage modules of the neat PSBA and corresponding PSBA/organo-MMT nanocomposite films.

Table V displays the results of nanoscratch test on the nanocomposite films, including mean nanoscratch groove depth and width, hardness, roughness, and grooving resistance. As shown, organoclay-reinforced copolymers exhibited a smaller nanoscratch groove depth, width, and roughness when compared with the neat copolymer. In contrast, the organoclay mainly increased the near-surface hardness and nanoscratch resistance in the nanocomposite films. As earlier mentioned, the molecular weight in the neat copolymer and its nanocomposite samples are almost the same to compare the effect of organoclay type and level on the nanoscratch behavior of copolymer. Thus, adding the high-modulus layered silicate material improved the

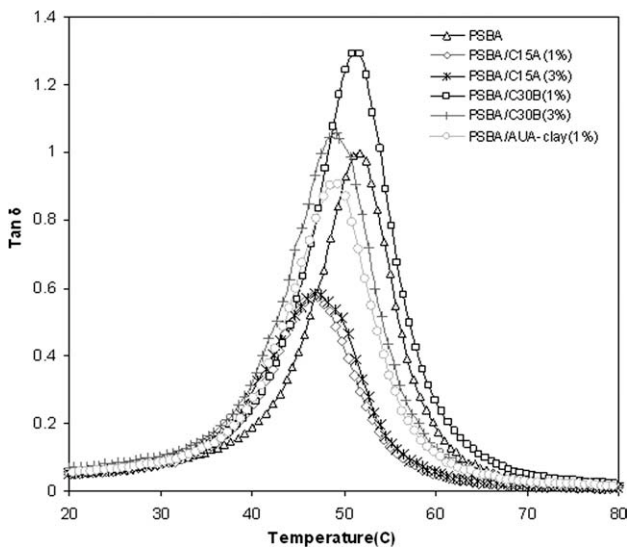

Figure 7 tan δ damping function variation vs. temperature for the neat and organo-MMT-reinforced PSBA.

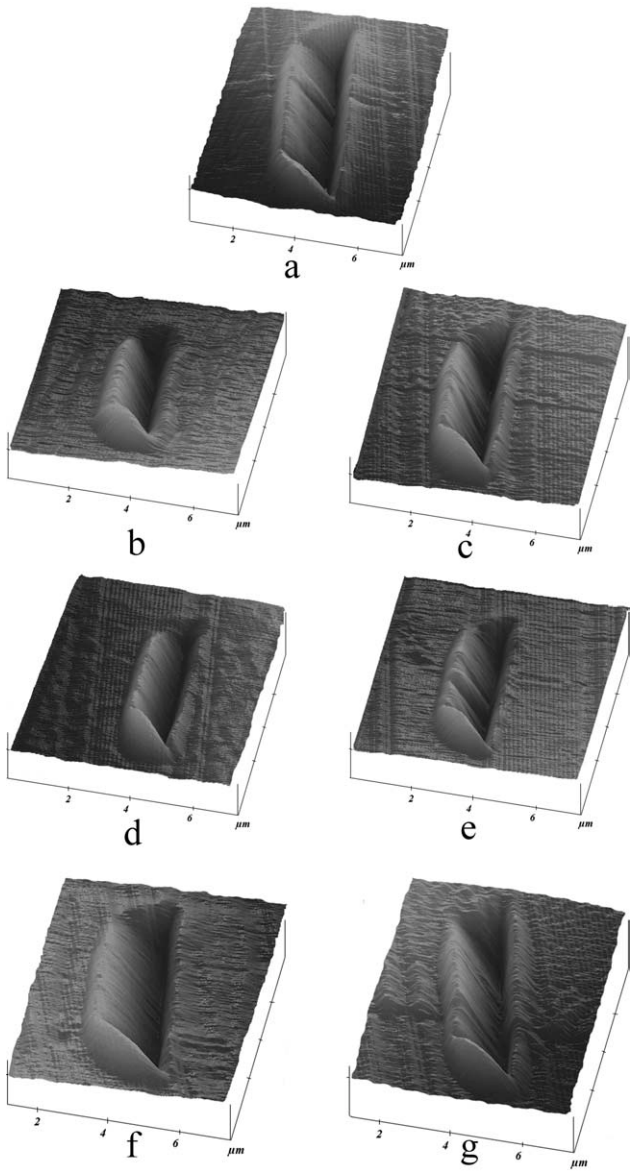

Figure 8 AFM phase image of nanoscratching of (a) neat PSBA and PBSA/organo-MMT nanocomposite samples containing: (b) 1 wt % C15A, (c) 3 wt % C15A, (d) 1 wt % C30B, (e) 3 wt % C30B, (f) 1 wt % AUA-Clay, and (g) 3 wt % AUA-Clay (The applied normal load was 150 μ*N*).

nanoscratch properties in the PSBA/organoclay nanocomposites. The lowest groove depth was observed for the nanocomposite films containing 1 wt % C30B and 3 wt % C15A for the applied normal loads 150 and 250 μ*N*, respectively. On the other hand, the increase of C15A organoclay level from 1 to 3 wt % enhanced considerably the hardness from 10.9 to 20.4 kg/mm^2, and nanoscratch resistance from 444.4 to 463.8 μJ/m at an applied normal load of 250 μ*N*. Deterioration of nanoscratch resistance property was observed for the PSBA/AUA-clay nanocomposites with a marked decrease in near-surface hardness and tanδ dissipation factor (Table V and Fig. 8). The increase of these two material

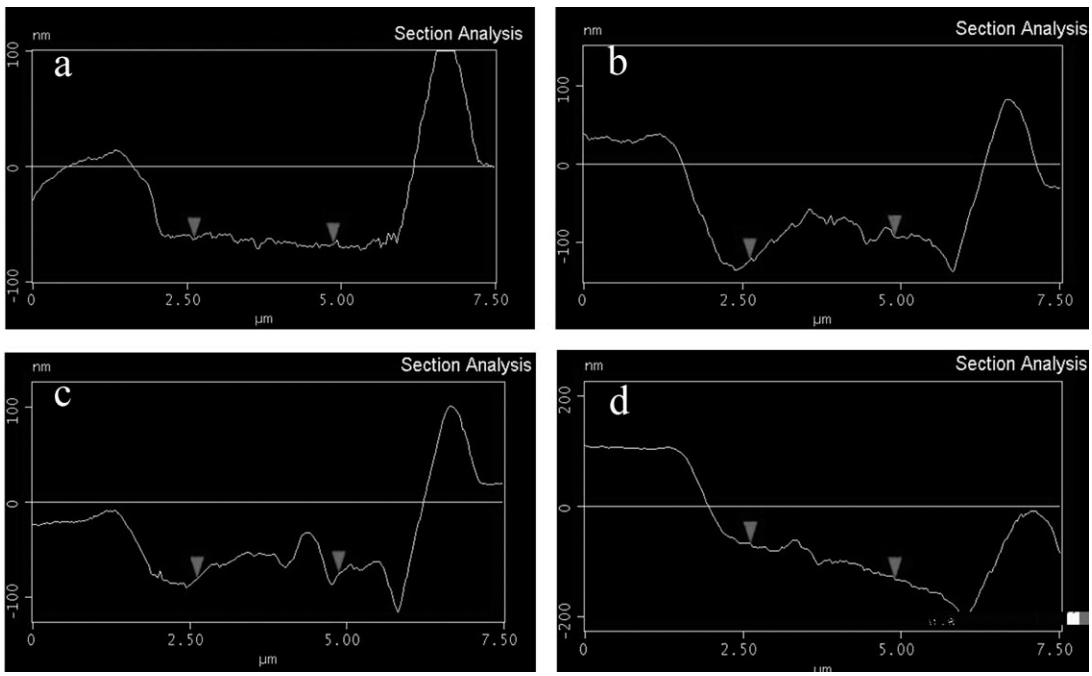

Figure 9 Residual depth of nanoscratch groove of (a) neat PSBA and PSBA-reinforced with 1 wt %: (b) Closite15A, (c) Closite30B, and (d) AUA-Clay (The applied normal force was 150 μ*N*).

properties seems to be an important parameter to improve the scratch resistance of the nanocomposite films without creating a bigger groove. On the other hand, lower aspect ratios in the range of 1.6–3.2 (Table IV), and poor dispersion of AUA-Clay layered silicates inside copolymer matrix [Fig. 5(e)] may induce high stress concentration around the particles, which facilitate the crack growth and make the matrix more brittle.

CONCLUSIONS

The effects of organic modifier type and level of organoclay, 1 and 3 wt %, have been investigated on the characteristics and mechanical properties of the resulting PSBA/organo-MMT nanocomposites prepared by *in situ* emulsion polymerization. The XRD patterns and TEM micrographs showed an intercalated nanocomposite structure for all the organoclay-reinforced copolymers. Although a uniform dispersion of dispersed organoclay particles was observed for the nanocomposites containing 1 wt % organoclay, the incorporation of 3 wt % organoclay caused particle agglomeration to occur, especially for the nanocomposite with AUA-clay. On the other hand, the incorporation of C15A organoclay in the structure of resultant hybrid latex particles decreased the mean particle size, while more hydrophilic organoclays, C30B and AUA-Clay, increased the size of hybrid particles. A decrease in the glass-storage modulus and glass-rubber transition temperature with a lower damping function (tan δ) were obtained as the organoclay added to the copolymer matrix.

Moreover, adding organoclay to the copolymer increased the near-surface hardness and grooving

TABLE V
Nanoscratch Characteristics of the PSBA/Organo-MMT Nanocomposite Films

Sample	Depth (nm)	Width (μm)	Hardness (kg/mm^2)	Roughness (nm)	Scratch resistance (μJ/m)
PSBA	218 (271)	1.26 (1.54)	12.0 (13.4)	25.9 (39.2)	199.6 (436.6)
PSBA/15A(1%)	187 (172)	1.16 (1.71)	14.2 (10.9)	15.3 (28.9)	216.4 (444.4)
PSBA/15A(3%)	171 (222)	1.07 (1.25)	16.7 (20.4)	12.3 (24.8)	273.6 (463.8)
PSBA/30B(1%)	183 (269)	1.15 (1.68)	14.5 (11.3)	15.0 (27.4)	237.5 (437.0)
PSBA/30B(3%)	160 (238)	1.05 (1.37)	17.3 (17.0)	10.1 (25.9)	273.8 (455.9)
PSBA/AUA(1%)	209 (300)	1.23 (1.80)	12.6 (9.8)	16.2 (31.7)	188.7 (412.0)
PSBA/AUA(3%)	172 (245)	1.10 (1.46)	15.8 (14.9)	12.8 (26.3)	262.8 (449.6)

[a] Amounts of scratch characteristics inside and outside the parentheses are related to the higher and the lower normal loads applied in the nanoscratch test.
[b] Scratch resistance was measured on the basis of the required energy to create a nanoscratch groove length of 5 μm.

resistance of the resulting nanocomposite films, while decreased the groove depth and the width as well as the residual surface roughness. The lowest groove depth was observed for the nanocomposite films containing 1 wt % C30B and 3 wt % C15A for the applied normal loads of 150 and 250 μ*N*, respectively. On the other hand, the introduction of 3 wt % C15A in the copolymer increased considerably the near-surface hardness from 13.4 to 20.4 kg/mm^2, and nanoscratch resistance from 436.9 to 463.8 μJ/m under an applied normal load of 250 μ*N*. The nanocomposite films with higher near-surface hardness and broader tan δ curve seem to have a higher grooving resistance against nanoscratching.

References

1. Ray, S. S.; Okamoto, M. Prog Polym Sci 2003, 28, 1539.
2. Tjong, S. C. Mater Sci Eng R 2006, 53, 73.
3. Pavlidou, S.; Papaspyrides, C. D. Prog Polym Sci 2008, 33, 1119.
4. Nayak, R. R.; Lee, K. Y.; Shanmugharaj, A. M.; Ryu, S. H. Eur Polym J 2007, 43, 4916.
5. Mu, M.; Walker, A. M.; Torkelson, J. M.; Winey, K. I. Polymer 2008, 49, 1332.
6. Wang, Z. Z.; Gu, P.; Zhang, Z. Wear 2010, 269, 21.
7. Aso, O.; Eguiazábal, J. I.; Naziabad, J. Comp Sci Tech 2007, 67, 2854.
8. Lertwimolnun, W.; Vergnes, B. Polymer 2005, 46, 3462.
9. Turri, S.; Torla, L.; Pccinini, F.; Levi, M. J Appl Polym Sci 2010, 118, 1720.
10. Choi, Y. S.; Ham, H. T.; Chung, I. J. Chem Mater 2004, 16, 2522.
11. de Paiva, L. B.; Morales, A. R.; Díaz, F.R.V. Appl Clay Sci 2008, 42, 8.
12. Li, H.; Yu, Y.; Yang, Y. Eur Polym J 2005, 41, 2016.
13. Kim, Y. K.; Choi, Y. S.; Wang, K. H.; Chung, I. J. Chem Mater 2002, 14, 4990.
14. Choi, Y. S.; Xu, M.; Chung, I. J. Polymer 2003, 44, 6989.
15. Kim, Y. K.; Choi, Y. S.; Wang, K. H.; Chung, I. J. Chem Mater 2002, 14, 4990.
16. Zhang, J.; Wilkie, C. A. Polym Degrad Stabil 2004, 83, 301.
17. D. Yei, R.; Kuo, S. W.; Su, Y.-C.; Chang, F. C. Polymer 2004, 45, 2633.
18. Aphiwantrakul, S.; Srikhirin, T.; Triampo, D.; Putiworanat, R.; Limpanart, S.; Osotchan, T.; Udomkichdecha, W. J Appl Polym Sci 2005, 95, 785.
19. Li, H.; Yu, Y.; Yang, Y. Eur Polym J 2005, 41, 2016.
20. Zhanga, R.; Hua, Y.; Xua, J.; Fana, W.; Chen, Z. Polym Degrad Stabil 2004, 85, 583.
21. Zhang, R.; Hu, Y.; Xu, J.; Fan, W.; Chen, Z.; Wang, Q. Macromol Mater Eng 2004, 289, 355.
22. Sahoo, P. K.; Samal, R. Polym Degrad Stabil 2007, 92, 1700.
23. Moraes, R. P.; Santos, A. M.; Oliveira, P. C.; Souza, F. C. T.; Amaral, M. D.; Valera, T. S.; Demarquette, N. R. Macromol Symp 2006,106.
24. Li, X; Gao, H.; Scrivens, W. A.; Fei, D.; Xu, X.; Sutton, M. A. Nanotechnology 2004, 15, 1416.
25. Liu, T.,Phang, I. Y.; Shen, L.; Chow, S. Y.; Zhang, W. D. Macromolecules 2004, 37, 7214.
26. Nai, M. H.; Lim, C. T.; Zeng, K. Y.; Tan, V. B. C. J Metastab Nanocryst Mater 2005, 23, 363.
27. Recco, A. A. C.; Viáfara, C. C.; Sinatora, A.; Tschiptschin, A. P. Wear 2009, 267, 1146.
28. Amerio, E.; Fabbri, P.; Malucelli, G.; Messori, M.; Sangermano, M.; Taurino, R. Prog Org Coat 2008, 62, 129.
29. Amerio, E.; Fabbri, P.; Malucelli, G.; Messori, M.; Sangermano, M.; Taurino, R. Prog Org Coat 2008, 62, 129.
30. Thridandapani, R. R.; Mudaliar, A.; Yuan, Q.; Misra, R. D. K. Mater Sci Eng 2006, A418, 292.
31. Dasari, A.; Yu, Z.-Z.; Mai, Y.-W. Acta Materialia 2007, 55, 635.
32. Bar, G.; Ganter, M.; Brandsch, R.; Delineau, L. Langmuir 2000, 16, 5702.
33. Remiro, P. M.; Marieta, C.; Riccardi, C. C.; Mondragon, I. Polymer 2001, 42, 9909.